

## Stress distribution during a silo filling or a discharging process

Ismain BABA AHMED<sup>a</sup>, Blaise NSOM<sup>b</sup>, Amine M ALLAL<sup>a</sup>, Fouad GHOMARI<sup>a</sup>

<sup>a</sup>Université Aboubekr Belkaid, BP 119 Tlemcen, Algérie

<sup>b</sup>Université de Bretagne Occidentale, Rue Kergoat 29231 Brest Cedex 3, France

---

### Abstract

The exploitation of the silos requires an accurate knowledge of the problems related to the processes of storage and discharge. The physical and mechanical characteristics of bulk material can be measured and controlled. Meanwhile, a bad management of the interaction between these characteristics and the storage conditions can give rise to a poor performance of the silo (flow rate during discharging, arching, etc.), or a failure of the structure. In order to investigate the principal disorders which can be observed during a filling and a discharge operation, the stress transmission within bulk materials is characterized with the help of discrete numerical simulations.

**Keywords:** Cell-hopper junction, Distinct Element Method, Discharging, Discrete simulations, Filling, Granular material, Silo, Stress transmission

---

### 1. Introduction

Nowadays, different methods and systems are available to silos designers and operators which aim at analyzing pressure on silos walls [1], [2]. Meanwhile, technological risks such as structure failure or formation of steady arches capable of blocking the operation subsist during a silo emptying process [3]. These defects are caused by the interaction between the physical and mechanical characteristics of the grains and matters in bulk [4] with the geometrical and mechanical characteristics of the silo and with the storage conditions [5]-[7]. The distribution of the forces exerting on a pile of dry grains is inhomogeneous. Certain grains are submitted to high stresses while other neighbouring ones support weaker stresses and may even be free to move [8]. Notably, an external stress applied to such a pile tends to follow paths involving touching particles. Moreover, increasing the external stress applied sets up an enrichment of the stresses paths involving a larger number of grains. In this way, ensiled grains tend to redirect the vertical stresses to the wall following given paths [2]. From Guiata et al. [9], one of the main causes for failure of grain silos is due to the excessive pressures exerted on the silo wall during discharge. Predicting how forces propagate into ensiled granular media is then a real scientific challenge with major industrial focus regarding the stockage and the handling of food grains. Continuous models give satisfactory results for the stress field within the silo at the end of the filling stage. Unfortunately, due to the large deformations which the ensiled matter undergoes, they require sophisticated rheological laws and numerical

methods as well, without meanwhile a reliable prediction of the kinematic field [10]. In contrast, Distinct Element Methods (DEM) which is based on a mechanical model of individual idealized particles and not on a continuum is more suitable to characterize the statistical distributions of contact forces inside the ensiled matter [11]. The DEM consist in tracking the motion of individual particles and updating any contact with neighbouring elements by using a constitutive contact law [12]. The program used in this work is PFC 2D (Particle Flow Code in two Dimensions) based on the DEM and the validation of the program is obtained by comparison with the results obtained by Masson and Martinez [12], [13] for similar configurations. A flat-bottomed and a cylinder-hopper silos are considered, the silo aspect ratio and the hopper slope being the geometric parameter in the simulations. While the grains are polydisperse, their number, diameter, density, friction angles (grain-grain and grain-wall), normal and tangential stiffness are the particle parameters.

### 2. The PFC 2D program

The particles used in the PFC 2D program are rigid disks which interact only at the contact of another particle or a solid wall. At the contact, the interaction induces an internal force which is responsible for an elastic deformation of the (nevertheless rigid) particle. The internal forces and the particles displacements are obtained by tracking the motion of each particle, itself produced by

the propagation of the perturbations throughout the granular system.

In this model, at a contact point of two particles, an interaction force is introduced which is proportional to their relative velocity and in opposite direction. Thus when two neighbouring particles get closer the interaction force has a repulsive effect; and when they move away one another, it has an attracting effect. This interaction force is modelled by a spring. An explicit time-difference scheme being applied on the interaction law, where the normal force  $(F_n)_t$  and the shear force  $(F_s)_t$  at a given contact point at time  $t$  are respectively given by:

$$(F_n)_t = (F_n)_{t-1} + \Delta F_n \quad (1)$$

$$(F_s)_t = (F_s)_{t-1} + \Delta F_s \quad (2)$$

where  $(F_n)_{t-1}$  and  $(F_s)_{t-1}$  are respectively the normal and the shear force at time  $t-1$  and  $(\Delta F_n, \Delta F_s)$  denotes the incremental normal and shear force, itself being given by:

$$\Delta F_n = k_n \Delta U_n + c_n v_n \quad (3)$$

$$\Delta F_s = k_s \Delta U_s \quad (4)$$

In these equations,  $k_n$  denotes the spring normal stiffness and  $c_n$  the normal damping coefficient, while  $\Delta U_n$ , the relative normal displacement is obtained by integration of the normal velocity by:

$$\Delta U_n = v_n \Delta t \quad (5)$$

Relations analogous to equations (3), (4) and (5) are written in the tangential direction. Newton's Second Law is then applied to a given particle with  $(\vec{r}_t, \varphi_t)$  polar coordinates at time  $t$  using the following relations, to determine its motion:

$$\vec{r}_{t+\Delta t} = \vec{r}_t + \dot{\vec{r}}_{t+\Delta t/2} \cdot \Delta t \quad (6)$$

$$\varphi_{t+\Delta t} = \varphi_t + \omega_{t+\Delta t/2} \cdot \Delta t \quad (7)$$

Where the translational and the rotational velocities are respectively given by:

$$\dot{\vec{r}}_{t+\Delta t/2} = \dot{\vec{r}}_{t-\Delta t/2} + \left[ \frac{\sum_i \vec{F}_t^i}{m} + \vec{g} \right] \Delta t \quad (8)$$

$$\omega_{t+\Delta t/2} = \omega_{t-\Delta t/2} + \left[ \frac{\sum_i M_t^{3i}}{I} \right] \Delta t \quad (9)$$

In these equations,  $\sum_i \vec{F}_t^i$  and  $\sum_i M_t^{3i}$  respectively denote the summation of all the forces and momenta in the  $z$ -direction (perpendicular to the plane of the motion), applied to the particle at time  $t$ , while  $m$  is the particle mass,  $I$  its moment of inertia and  $\vec{g}$  the gravity and  $\Delta t$  is the time step. Finally, it should be noticed that a discrepancy exists in the literature between the values used for the different model parameters:  $c_n$ ,  $c_s$ ,  $k_n$  and  $k_s$  (e.g.: Tsuji and Oikawa, among others [14]).

### 3. Digital Simulation

The granular flows are generally classified in three distinct modes: the quasi-static mode, the dense mode and the collision mode. In the quasi-static mode the movement of the particles is relatively slow or non-existing, while the granular matter is driven as a liquid in the dense mode, and as gas atoms in the collision mode [15]. In the quasi-static mode of a grain flow inside a silo, the bulk material is in constant disturbance at each filling or discharge operation with statement that the material reaches the threshold of rupture to each use of the silo, which gives rise to the following fundamental question: how are distributed the strains and the stresses once this threshold is exceeded? It is especially a problem of including/understanding this evolution at the contact of the matter with the walls of the silo, since it is in this zone that the slip occurs. Indeed the slip of the grains both on the other grains and on the walls is the main parameter for the understanding of such phenomena as the sticking or the stress peaks located at the cell-hopper junction. In this work, we will focus on cylindrical vertical silos, where two flow types can be identified: the mass flow, characterized by sufficiently steep and smooth walls of the hopper and the funnel flow when they are gently sloping and rough [16]-[19]. The characteristics of the simulated matters are presented in Tables 1 & 2, while the procedure of the simulation is

presented in Figure 1. In these simulations, abroad the required traditional goals such as the stress field and the strain field at special locations where the studied poor running phenomena take place inside the silo, we quantify the parameters specific to the granular materials such as the coordination number, the contact forces, etc. The simulation of a silo filling and discharging was performed using a DEM software PFC 2D, suitable for a 2D numerical modelling of discontinuous media.

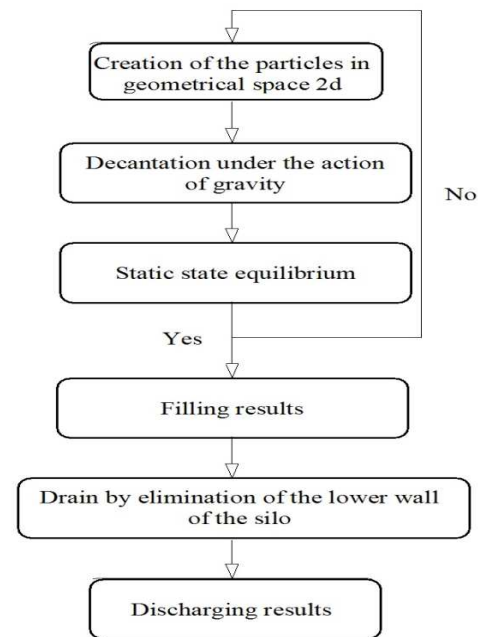


Fig. 1. Procedure used for the simulations.

Table 1

Input data for a flat bottom silo

1 <sup>st</sup> case	Grain-Grain	Grain-Wall
Density of material	1.607	-
Angles of Friction	$\Phi_G=45^\circ$	$\Phi_P=26,5^\circ$
Normal & tangential stiffness	$K_n=50\ 000\text{N/m}$ $K_s=1\ 000\text{N/m}$	$K_n=50\ 000\text{N/m}$ $K_s=1\ 000\text{N/m}$
Rays of grains	$0.09\text{m}<r<0.11\text{m}$	$0.09\text{m}<r<0.11\text{m}$

Table 2

Input data for a conical Hopper

2 <sup>nd</sup> case	Grain-Grain	Grain-Wall
Density of material	0.835	-
Angles of Friction	$\Phi_G=25^\circ$	$\Phi_P=24^\circ$
Normal & tangential stiffness	$5\ 10^6\ \text{N/m}$	$5\ 10^6\ \text{N/m}$
Rays of grains	$0.09\text{m}<r<0.11\text{m}$	$0.09\text{m}<r<0.11\text{m}$

Table 3

Coordination number for different grain shape

Grain shape	Parameters	$C_n$
Convex Grains	Circular Grains net square, equal ray	4
	Circular Grains net triangular, equal ray	6
	Circular Grains "random ray"	$\sim 4$
	Intergranular Vacuum Triangular	4
	Intergranular Vacuum Unspecified	$\leq 6$
Non convex Grains	Vacuum in no triangular form with curvilinear edge	Unlimited

#### 4. Results of the Simulation

A pile of grains is characterized by a network of contact which transmits the forces. The random aspect of the distribution of the chains of forces was reduced to statistical approaches taking into account the number of average contacts per grain, also called coordination number [20].

##### 4.1. Coordination Number

If  $n_c$  denotes the number of contacts per particle and  $N$  the number of particles in the defined measuring space  $V$  (closer to the desired calculated zone), the coordination number  $C_n$  is defined as

$$C_n = \frac{\sum n_c}{N_p} \quad (10)$$

The geometrical shape of these grains is essential to characterize the sample studied. Tables 1-2 present the different mechanical and geometrical characteristics of the silo and those of the granular material studied and Table 3, the coordination number for different grain shapes.

Figures 2a-2b presents the evolution of the coordination number against the number of cycles for the target of our digital simulations. It is computed at the cell-hopper junction, using the Cundall model [11].

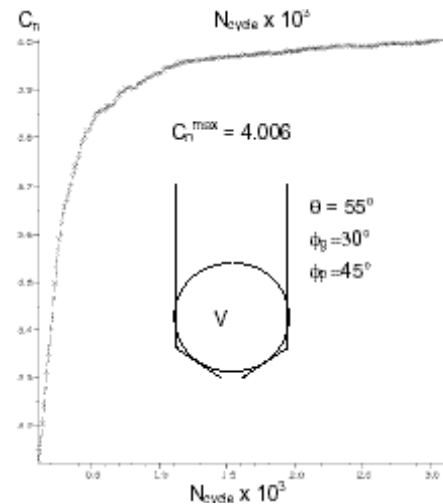


Fig. 2a. Coordination number in a sample space

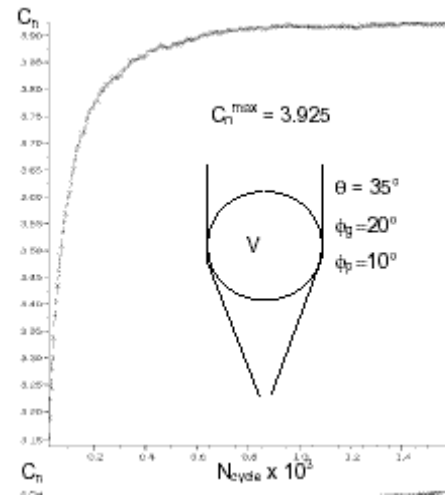


Fig. 2b Coordination number in a sample space

##### 4.2 Pressure on the walls during a filling operation

The vertical and the horizontal stresses on the silo walls can be calculated using eqs. (11) - (12). Their variation along the silo vertical wall is shown in Figures 3.a and 3.b, respectively, after a filling operation. In each of these figures, the pressures exerted by the grains on the silo walls using the equations given above are called the Janssen equations [21].

$$\sigma_v = \frac{\rho g R}{2K\mu_s} \left\{ 1 - \exp \left[ \frac{(z-h)2K\mu_s}{R} \right] \right\} \quad (11)$$

$$\sigma_H = \gamma \left[ \frac{h'-z}{n_i} + \left( \frac{q}{\gamma} \frac{h'}{n_i} \right) \left( 1 - \frac{z}{h'} \right)^{n_i+1} \right] \quad (12)$$

In these equations,  $\rho$  is the matter density,  $g$  the gravity,  $\gamma = \rho g$  the unit weight,  $R$  the radius of the silo cell,  $K$  the Janssen coefficient (equal here to 0.4 during a filling

operation and between 0.25 and 0.6 during a discharge),  $\mu_s$  the grain/wall static friction coefficient,  $h$  the cell height,  $h'$  the hopper height,

$$n_i = 2 \left( 1 + \frac{\tan \Phi_P}{\tan \theta} \right)^{-3}$$
 a parameter where  $\Phi_P$  denotes the grain/wall friction angle and  $\theta$  the hopper slope;  $z$  the vertical coordinate and finally  $q = \frac{\sigma_H}{K}$  a part of the horizontal stress.

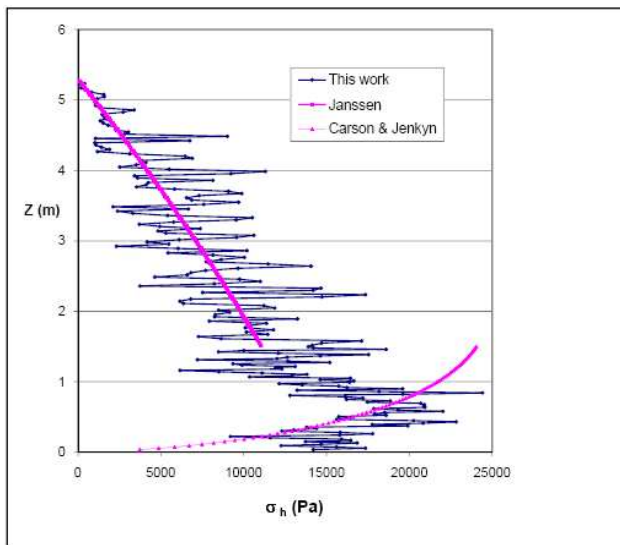


Fig. 3a Variation of horizontal stress along silo vertical wall

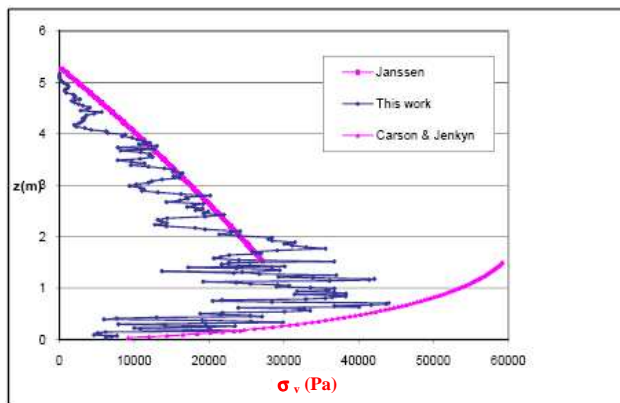


Fig. 3b Variation of Vertical stress along silo vertical wall

These curves show a satisfactory agreement in the vertical part of the silo ( $1.5\text{m} < z < 5.3\text{m}$ ), and on the lower two thirds of the hopper ( $0 < z < 0.8\text{m}$ ). Moreover, a disturbance of the vertical and the horizontal stress can be noticed on the right part of the cell-hopper junction ( $0.8\text{m} < z < 1.5\text{m}$ ). This phenomenon defines the “switch zone” where depressure (or overpressure) take place either in a geometrical silo

walls (silo hopper in Figure. 4a) or fictitious and random walls materialized by the intersecting lines between the dead zones and the flow zones inside the matter (flat-bottom silo, Figure 4.b). The stress peak is a direct consequence of this perturbation. The discrepancy which characterizes the values of the stress obtained in these curves can be interpreted. Indeed it clearly shows that the studied medium must not be regarded as a continuous medium, but as discontinuous medium. This matter of fact completely justifies the use of a DEM [22]. By withdrawing the lower wall of the silo, a discharging takes place and as from the first case, we notice the amplification of the network of the contact forces to the altitude of  $+3.00\text{ m}$  Figure 5. The variation of the stress along the vertical wall is plotted on Figure 6, and it clearly shows the peak of stress on the right of the top of the dead zone and has as a value of  $22\,960\text{ Pa}$ , in horizontal stress [23], [24].

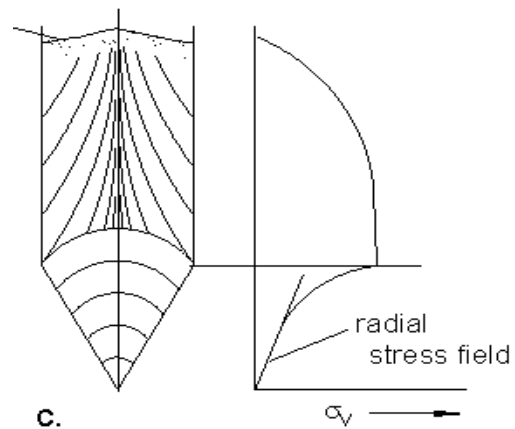


Fig. 4a Stress increasing in switch zone

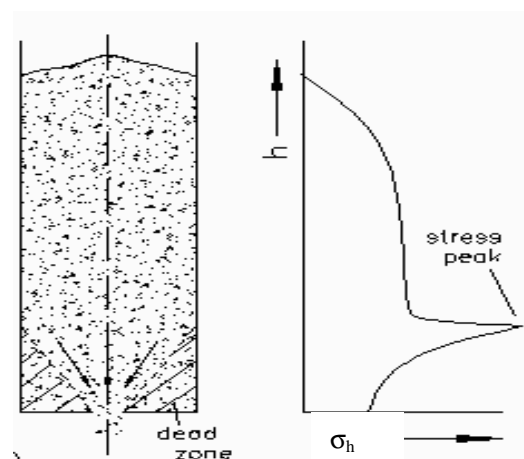


Fig. 4b Stress decreasing in switch zone

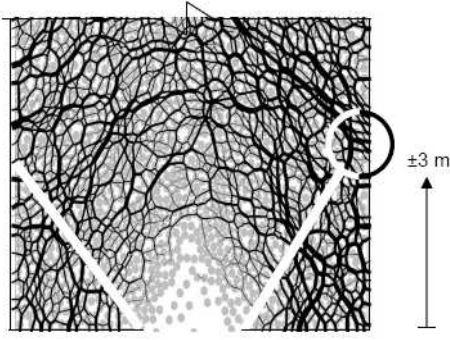


Fig. 5 Intergranular force network (silo 2; K=0.4)

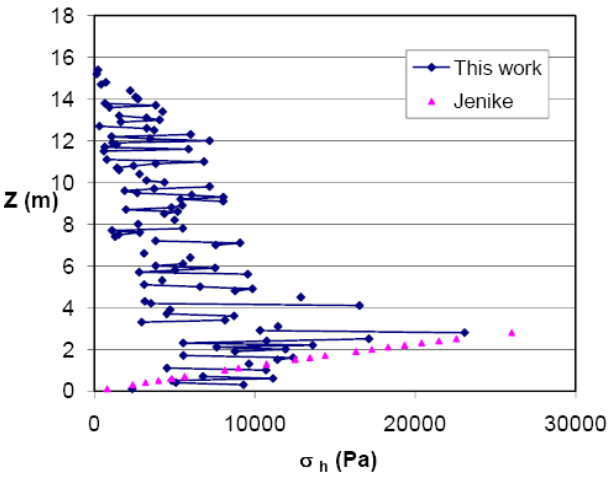


Figure 6: Horizontal stress on the edge (silo 2; K=0.4)

## 5. Parametric study

The mechanical parameters as measurable quantities are important for the transmission of the stress. Their introduction as micromechanical variables into a digital model, using a DEM, can account for the influence which they have on the macroscopic mechanical behaviour of a granular medium. The parametric study was performed with respect to the two following mechanical parameters of the ensiled medium: the grain-grain friction and the grain-wall friction, while the geometric silo parameter is the slope of its hopper walls. The other parameters such as the material density, the grain stiffness and the silo walls roughness, the silo height  $H$ , the aperture as well as the grain size are kept constant. The different results obtained are expressed in terms of force network, evolution of horizontal and vertical stress (Figures 7a, 7b, 7c) as well as their ratio, given by equations (10) et (11).

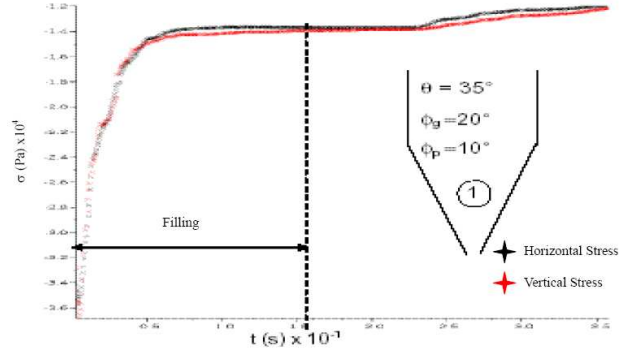


Fig. 7a Evolution of horizontal and vertical stress during silo use (case 1)

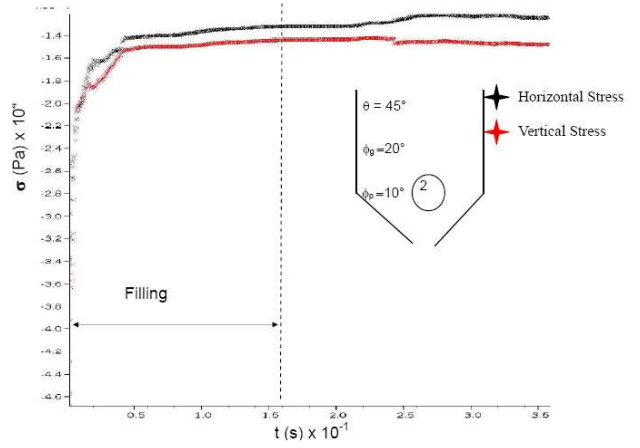


Fig. 7b Evolution of horizontal and vertical stress during silo use (case 2)

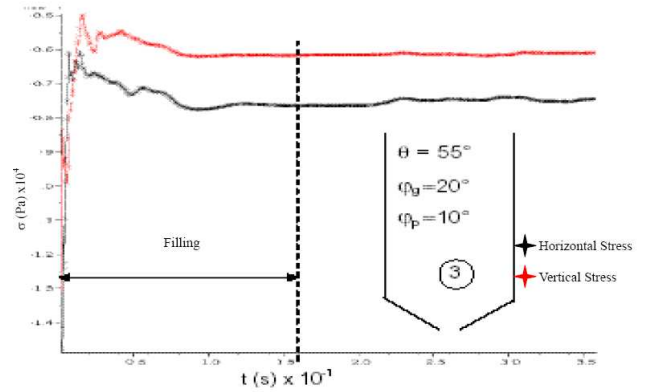


Fig. 7c Evolution of horizontal and vertical stress during silo use (case 3)

The stress distribution can also be shown by drawing the variation (increasing or decreasing) of the stresses using percentage bars with respect to their values during the filling operation (figs. 8a and 8b). In fig. 8a we can see that the horizontal stress increasing is more important for

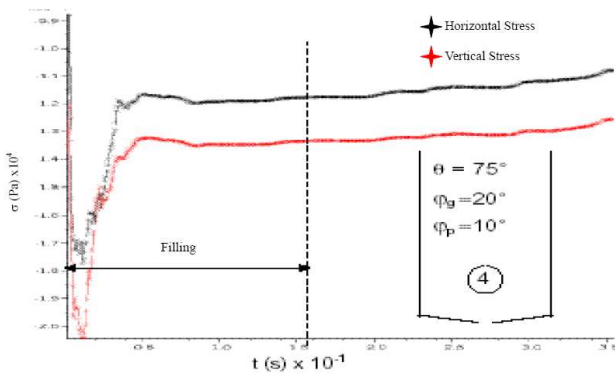


Fig. 7d Evolution of horizontal and vertical stress during silo use (case 4)

hoppers with a slope of  $35^\circ$  and  $45^\circ$  with low values of  $\phi_g$  ( $20^\circ$  and  $30^\circ$ ) than for hoppers with a slope of  $55^\circ$  where a decreasing is noticed. The exception of a hopper with a slope of  $75^\circ$  give opposite results as the increasing obtained is as important as in the three previous hoppers (about 9% for  $\phi_p = 10^\circ$ ). While for the vertical stresses, the increasing is much more for the hopper with a slope of  $35^\circ$  whatever the grain-grain and grain-wall frictions are. The increasing for  $\theta = 45^\circ$ ,  $55^\circ$  and  $75^\circ$  with  $\phi_p = 10^\circ$ ,  $\theta = 55^\circ$  and  $75^\circ$  with  $\phi_p = 45^\circ$  are also negative. This result confirms the horizontal transmission of the stresses. So the geometric parameter «hopper slope  $\theta$ » has a clear influence on the values of the horizontal and the vertical stresses at the switch zone. Slopes lower than  $45^\circ$  produce an important increasing of the stresses and conversely, slopes higher than  $45^\circ$  produce a lower increasing of the stresses. These increasing cause no major safety risk for the design of the silos (failure or explosion of the structure), but their better understanding allow a better silo exploitation (avoidance of dead zones). The angles of friction parameters  $\phi_p$  and  $\phi_g$  have an influence on the stress transmission as they give to the ensiled matter, preferred orientations to the network of the contact forces. Masson & Martinez [25] obtained similar result with flat bottom silos with variable friction and stiffness. The ensiled matter has a variable behaviour according to the state of its use: under geometrical conditions such as conical silos of very strong slope and slightly hurled, it will run out relative at ease without too much increase in constraint. It will tend to have a behavior of continuous medium. On the other hand under conditions geometrical such as silos flat-bottomed and strongly slim, the granular matter will undergo a random state of stress causing of the notorious dysfunctions, like containment, the phenomenon of the vaults, etc.

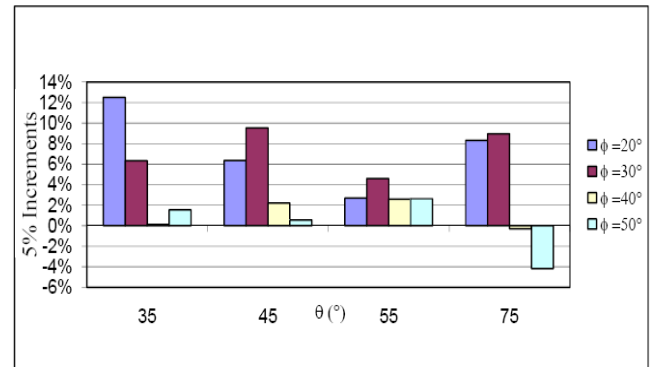


Fig. 8a Evolution of horizontal and vertical stress during silo use (case 4)

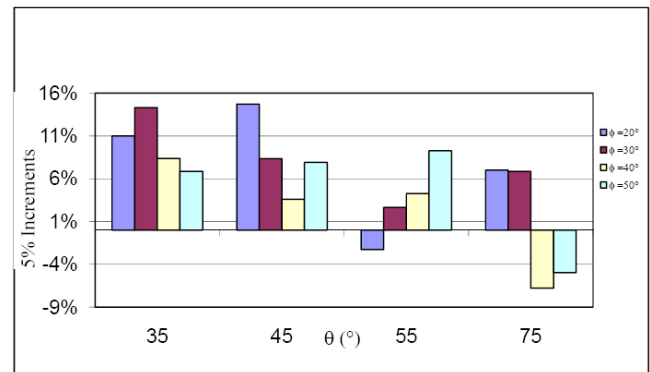


Fig. 8b Evolution of horizontal and vertical stress during silo use (case 4)

## 6. Conclusion

This paper considered the main observable phenomena during a filling and a discharging operation of a silo and their consequences on the bulk material behaviour. In particular, using direct numerical simulations, we addressed the pressure on the silo walls. We were able to observe a quite relationship between the form of the pressure curve of both horizontal and vertical stress values in the simulation and the real measurement on the silo obtained on other works [26], in spite of the smallest values of these stress value calculated on the simulation. Then a parametric study was performed and the time evolution of the pressure could be computed. The results we obtained for case 2 shown on figure 7b conclude to a nearly linear ratio of the horizontal stress to the vertical stress. This means that in the zone of cell-hopper junction, whatever the stress increasing could be, the mechanical behaviour of the granular material is similar to that of a continuous medium. In opposition, for case 4 on figure 7d, the fluctuations in this ratio are so high that the stress field is anisotropic.

## References

- [1] Reimbert, A. and Reimbert M. "Silos", eds Eyrolles, Paris (1956)
- Schulze D (2004), Storage of Powders and Bulk solids in silos, Eds (2004)
- [2] Jenike AW: Storage and flow of solids. Bull. N°123 (1964), Eng. Exp. Station, Univ. Utah, Salt lake City.
- [3] Brown CJ and Nielsen J: "Silos. Fundamentals of theory, behaviour and design", (1998) Eds. E & FNn SPON, London.
- [4] Degouet C, Nsom B, Lolive E & Grohens A: Characterization of Soya, Colza and Rye Seeds, Appl. 186 Rheol 17(3) (2006).365461-365467
- [5] Teunou E and Fitzpatrick JJ: Effect of storage time and consolidation on food powder flowability, J.Food Eng., 43 (2000) 97-101.
- [6] Fitzpatrick JJ, Iqbal T, Delaney C, Twomey T and Keogh MK: J. Food Eng. 64 (2004) 435-444.
- [7] Fitzpatrick JJ, Barringer SA & Iqbal T: Flow property measurement of food powders and sensitivity.
- [8] Claudin P: La physique des tas de sable (1999), EDP Sciences, Les Ulis (France)
- Cundall PA & Strack ODL: A discrete numerical model for granular assemblies. Geotech, 29 (1979) 18247-65.
- [9] Guaita M, Couto A & Ayuga F: Numerical Simulation of Wall Pressure During Discharge of Granular Material from Cylindrical Silos with Eccentric Hoppers. Biosystems Engineering 85 (2003) 101-109.
- [10] Masson S, Martinez J, Ferrelec JF & Parisi D: Simulation numérique discrète des écoulements granulaires confinés. Actes du 16ème Congrès Français de Mécanique (2003), Nice (France).
- [11] P.A. Cundall, O.D.L. Strack, A discrete numerical model for granular assemblies. Geotechnique (1979), 29:47-6.
- [12] Masson M & Martinez J: Multiscale simulations of the mechanical behaviour of an ensiled granular 209 material, Mech. Cohes-Frict. Mater. 5 (2000) 425-442.
- [13] Goda, T.J. & Ebert, F.: Three dimensional discrete element simulations in hoppers and silos. Powder Technology (2005), 158, 58-68.
- [14] Tsuji H & Oikawa M: Two Dimensionnel interaction of internal Solitary waves in a two layer Fluid. J.Phys. Soc. Japan, 62 (1993) 3881-3892.
- [15] GDR MiDi: Groupement De Recherche Milieux Divises, CNRS, GDR2181, On dense granular flow, The European Physical Journal E, 14 (2004) 341-365.
- [16] Degouet C, Nsom B, Lolive E & Grohens A: (2007). Image Processing for the Measurement of Flow Rate of Silo Discharge, in "Innovation and Advanced Techniques in Computer and Information".
- [17] Job, N., Dardenne, A. & Pirard, J-P: Silo flow-pattern diagnosis using the tracer method, J. Food Eng., 91(1) (2009), 118-125.
- [18] Chen, J.F., Rotter, J.M., Ooi, J.Y. & Zhong, Z.: Flow pattern measurement in full scale silo containing iron ore. Chem. Eng. Sci. (2005), 60(11), 3029-3041.
- [19] Ostendorf, M. & Schwedes, J.: Application of particle image velocimetry for velocity measurements during silo discharge. Powder Technology (2005), 158, 69-75
- [20] Weber JD: (1966). Recherches concernant les contraintes intergranulaires dans les milieux pulvérulents. Bulletin de liaison Laboratoire des Ponts et chaussées, 337 (1966) 3-1,3-19.
- [21] Jenike's hopper design methodology to the measured values. J. Food Eng. 61 (2004) 399-405.
- [22] Müller D: Techniques efficaces pour la simulation de milieux granulaires par la méthode des éléments distincts, Thèse de Doctorat, N°1545 (1996) EPFL, Switzerland (in French),
- [23] Ismain Baba Ahmed, B. Nsom, M. Allal et F.Ghomari: "Behaviour of Granular Material During a Silo Filling or Gischarging", Proceedings of the 2nd ICMS (International Conference on Mechanical Sciences), Oum El Bouaghi, Algeria (2008)
- [24] Ismain Baba Ahmed, B. Nsom, M. Allal et F.Ghomari: " Rheology and Structure of Ensiled Food Grains", Proceedings of the 5th ISFRS (International Symposium on Food Rheology and Structure), Zurich, Suisse (2009).
- [25] Masson M & Martinez J: Effect of particle properties and silo geometry on stresses predicted by discrete simulations of bulk materials. Proceedings EM02, ASCE (2002), New York.
- [26] Carson JW & Jenkyn RT: "How to explore prevent silo failure with Routine Inspections and Proper 179 Repair", Powder and Bulk Engineering, Vol. 4 (1990) 18-23.